NASA TECHNICAL NOTE

NASA TN D-5455



NASA TN D-5455

# CALCULATION OF THE PENETRATION FLUX FOR A MULTIWALL STRUCTURE ON THE LUNAR ORBITER SPACECRAFT

*by Donald H. Humes*

*Langley Research Center*
*Langley Station, Hampton, Va.*

NATIONAL AERONAUTICS AND SPACE ADMINISTRATION • WASHINGTON, D. C. • NOVEMBER 1969

| | | |
|---|---|---|
| 1. Report No.<br>NASA TN D-5455 | 2. Government Accession No. | 3. Recipient's Catalog No. |
| 4. Title and Subtitle<br>CALCULATION OF THE PENETRATION FLUX FOR A MULTIWALL STRUCTURE ON THE LUNAR ORBITER SPACECRAFT | | 5. Report Date<br>November 1969<br>6. Performing Organization Code |
| 7. Author(s)<br>Donald H. Humes | | 8. Performing Organization Report No.<br>L-6609<br>10. Work Unit No.<br>124-09-25-01-23 |
| 9. Performing Organization Name and Address<br>NASA Langley Research Center<br>Hampton, Va. 23365 | | 11. Contract or Grant No.<br>13. Type of Report and Period Covered<br>Technical Note |
| 12. Sponsoring Agency Name and Address<br>National Aeronautics and Space Administration<br>Washington, D.C. 20546 | | 14. Sponsoring Agency Code |

15. Supplementary Notes

16. Abstract

The method used to calculate the penetration flux for the Lunar Orbiter multiwall structure consisting of the thermal barrier and the photo-subsystem container is presented. The calculation of the efficiency factor showed that the multiwall structure provided better protection against meteoroids than a single aluminum wall with the same mass per unit area. The calculated efficiency factor was 5.9. The flight data from the five Lunar Orbiter missions verified that the multiwall structure was more effective than a single aluminum wall of the same mass per unit area, but the data were not adequate to determine the value of the multiwall efficiency factor.

| | |
|---|---|
| 17. Key Words Suggested by Author(s)<br>Meteoroids<br>Lunar Orbiter<br>Meteoroid bumper | 18. Distribution Statement<br>Unclassified – Unlimited |

| | | | |
|---|---|---|---|
| 19. Security Classif. (of this report)<br>Unclassified | 20. Security Classif. (of this page)<br>Unclassified | 21. No. of Pages<br>24 | 22. Price*<br>$3.00 |

*For sale by the Clearinghouse for Federal Scientific and Technical Information
Springfield, Virginia 22151

# CALCULATION OF THE PENETRATION FLUX FOR A MULTIWALL STRUCTURE ON THE LUNAR ORBITER SPACECRAFT

By Donald H. Humes
Langley Research Center

## SUMMARY

The method used to calculate the penetration flux for the Lunar Orbiter multiwall structure consisting of the thermal barrier and the photo-subsystem container is presented. The calculation of the efficiency factor showed that the multiwall structure provided better protection against meteoroids than a single aluminum wall with the same mass per unit area. The calculated efficiency factor was 5.9. The flight data from the five Lunar Orbiter missions verified that the multiwall structure was more effective than a single aluminum wall of the same mass per unit area, but the data were not adequate to determine the value of the multiwall efficiency factor.

## INTRODUCTION

An evaluation of the meteoroid hazard to the Lunar Orbiter spacecraft made prior to the spacecraft missions indicated that the photo-subsystem container on each spacecraft would have a 0.5 probability of being penetrated by a meteoroid during the 30-day photographic mission unless the thermal barrier, which was wrapped around the spacecraft frame, was an effective meteoroid bumper. A photograph of the Lunar Orbiter spacecraft showing the photo-subsystem container and a portion of the thermal barrier is presented in figure 1. The photo-subsystem container was pressurized and housed the camera, film, film processor, and other photographic components which could function properly only if the internal pressure was maintained. A meteoroid penetration of the photo-subsystem container would result in a loss of pressure which would cause the photo subsystem to be inoperative. The 0.5 probability of such an event occurring was an unacceptable risk, and an analysis was made to determine whether the thermal barrier would be an effective meteoroid bumper and would significantly reduce the probability of a meteoroid penetration through the photo-subsystem container.

Meteoroid bumper is the term that is usually applied to the outermost wall of a multiwall structure, and its function is to fragment impacting meteoroids so that the meteoroid damage is spread over a large area of the inner walls in the form of many

small craters. Laboratory tests indicate that the multiwall structures have a greater resistance to penetration by hypervelocity particles than single-wall structures with the same mass per unit area because the damage to a single wall is concentrated in one large crater.

The analysis showed that the thermal barrier would be an effective meteoroid bumper and that the penetration flux for the configuration of the thermal barrier and photo-subsystem container would be low. The probability that the photo-subsystem container would be penetrated by a meteoroid was determined to be less than 0.03 for the photographic mission of each spacecraft.

In this report, the method used to calculate the penetration flux for the configuration of the thermal barrier and photo-subsystem container is described and the resulting calculations are presented, some improvements being incorporated in both as a result of a more recent analysis. Also included in this report are the flight data on the penetration flux of the thermal barrier and photo-subsystem container obtained from the five Lunar Orbiter missions. The efficiency factor for the Lunar Orbiter multiwall structure is discussed as well as the number of penetrations that must be obtained in a flight experiment to check adequately methods of calculating penetration flux.

## SYMBOLS

| | |
|---|---|
| $A$ | area of spacecraft structure exposed to meteoroid environment |
| $E$ | efficiency factor for multiwall structure, $t_{eff}/t_{act}$ |
| $F_i$ | fraction of meteoroids with velocity in interval $\Delta V_i$ |
| $f(V)$ | penetration function for spacecraft structure which takes into consideration meteoroid mass and impact-velocity parameters |
| $f(\theta,\rho,V)$ | penetration function for spacecraft structure which takes into consideration meteoroid mass, impact-velocity, density, and impact-angle parameters |
| $g(V)$ | meteoroid impact-velocity probability density function |
| $h(\rho)$ | meteoroid density probability density function |
| $i(\theta)$ | meteoroid impact-angle probability density function |

| | |
|---|---|
| $K$ | number of penetrations |
| $k_1, k_2, k_3$ | constants |
| $m$ | mass of particle |
| $m_i$ | minimum-mass particle with velocity in interval $\Delta V_i$ which penetrates structure |
| $N$ | accuracy factor of calculated penetration flux |
| $P_o$ | probability of no meteoroid penetrations |
| $t$ | thickness of single-wall structure |
| $t_{eff}$ | effective thickness of multiwall structure |
| $t_{act}$ | actual thickness of all material in multiwall structure |
| $V$ | velocity of particle |
| $\Delta V_i$ | ith velocity interval |
| $\Delta V_n$ | nth velocity interval |
| $Z$ | error factor in calculated penetration flux, $\psi/\psi_c$ when $\psi > \psi_c$ and $\psi_c/\psi$ when $\psi_c > \psi$ |
| $\theta$ | impact angle |
| $\rho$ | particle mass density |
| $\tau$ | time of spacecraft exposure to meteoroid environment |
| $\phi$ | cumulative meteoroid flux |
| $\phi_i$ | cumulative flux of meteoroids of mass $m_i$ and greater |
| $\psi$ | actual mean penetration flux |

$\psi_c$ calculated penetration flux

$\psi_i$ calculated penetration flux of meteoroids with velocity in interval $\Delta V_i$

$\psi_L$ lower limit of 95-percent confidence interval for measured penetration flux

$\psi_U$ upper limit of 95-percent confidence interval for measured penetration flux

$\psi_{dm,dV}$ calculated penetration flux of meteoroids with mass in interval $dm$ and velocity in interval $dV$

Subscripts:

i ith interval

max maximum

min minimum

n nth interval

## ANALYSIS

### Method of Calculating Penetration Flux for a Multiwall Structure

The method used to calculate the penetration flux for the thermal barrier and photosubsystem container consists of a penetration criterion for the multiwall structure and a description of the meteoroid environment. The penetration criterion is expressed in terms of the minimum meteoroid mass which penetrates the structure as a function of the impact velocity. The meteoroid environment is described by two distributions: the distribution of meteoroid masses and the distribution of meteoroid velocities.

The method of calculating the penetration flux for a multiwall structure is illustrated in figure 2. The minimum-mass curve in figure 2 defines the joint conditions of mass and velocity which a meteoroid must have to penetrate the structure. The lethal conditions are those above the minimum-mass curve. The flux of meteoroids which have a mass in the interval $dm$ and a velocity in the interval $dV$ is

$$\psi_{dm,dV} = \frac{\partial \phi}{\partial m} g(V)\, dm\, dV$$

where $\partial\phi/\partial m$ is the differential mass-flux distribution function and $g(V)$ is the meteoroid impact-velocity probability density function. The total calculated penetration flux $\psi_c$ for the structure is

$$\psi_c = \int_{V=0}^{\infty} \int_{m=f(V)}^{\infty} \frac{\partial \phi}{\partial m} g(V)\, dm\, dV \tag{1}$$

where $m = f(V)$ is the penetration criterion for the structure.

A numerical method for performing the integration in equation (1) is illustrated in figure 3. Figures 3(b) and 3(c) are the mass and velocity distributions of meteoroids in the form in which they are most often expressed. Figure 3(b) is the cumulative mass-flux curve; that is, the number of meteoroids of a given mass or greater that strike a unit area in a unit time. Figure 3(c) is the normalized frequency distribution of meteoroid velocities presented as a histogram. To calculate the penetration flux, consider one of the velocity intervals $\Delta V_i$ in which a fraction $F_i$ of the meteoroid population falls. At a velocity representative of the interval $\Delta V_i$, a mass $m_i$ is the minimum mass that penetrates the structure. All meteoroids with a mass greater than $m_i$ and a velocity in the interval $\Delta V_i$ penetrate the structure. The flux of meteoroids with a mass of $m_i$ and greater is $\phi_i$, but this flux is for meteoroids of all velocities. If the mass distribution and velocity distribution are independent, the calculated penetration flux for meteoroids in the velocity interval $\Delta V_i$ is

$$\psi_i = F_i \phi_i \tag{2}$$

and the total calculated penetration flux $\psi_c$ for meteoroids of all velocities is

$$\psi_c = \sum_{i=1}^{n} F_i \phi_i \tag{3}$$

where $n$ is the total number of velocity intervals. The penetration flux for the configuration of the thermal barrier and photo-subsystem container was calculated by using this numerical method.

## Description of Lunar Orbiter Multiwall Structure

The multiwall structure considered in this report is the configuration of the thermal barrier and photo-subsystem container on the Lunar Orbiter spacecraft. A sketch of this multiwall structure is presented in figure 4.

The thermal barrier, which was the outermost wall or meteoroid bumper, consisted of alternate layers of aluminized plastic film and dacron scrim leno weave and had a mass per unit area of about 0.014 g/cm$^2$ and a total thickness of about 0.8 mm. The primary function of the thermal barrier was to provide passive thermal control for the photo subsystem. The photo-subsystem container was the inner wall of the multiwall structure. It was a 0.4-mm-thick pressurized aluminum container with a surface area of about 1.4 meters$^2$.

The thermal barrier was separated from the photo-subsystem container by a distance of about 0.1 meter at the nearest point and a distance of about 0.6 meter at the farthest point, the average distance being about 0.4 meter. This multiwall structure had a total mass per unit area of 0.125 g/cm$^2$ and a 1 to 8 distribution of the mass per unit area between the bumper and the main wall.

## Application of Method of Calculating Penetration Flux for a Multiwall Structure to the Lunar Orbiter Multiwall Structure

The penetration flux for the configuration of the thermal barrier and photo-subsystem container on the Lunar Orbiter Spacecraft was calculated by using the numerical method outlined in figure 3. Before the calculation could be performed, it was necessary to establish the penetration criterion for the multiwall structure expressed in terms of the minimum mass which penetrates the structure as a function of the impact velocity. It was also necessary to describe the meteoroid environment encountered by Lunar Orbiter by the distribution of meteoroid masses and the distribution of meteoroid velocities.

The penetration criterion for the structure was based on laboratory data obtained in hypervelocity impact ranges in which the Lunar Orbiter multiwall structure and other multiwall structures were used as targets.

Laboratory tests conducted in hypervelocity impact ranges have provided data on the minimum mass which penetrates a double-wall structure for impact velocities up to about 8 km/s. The minimum mass that penetrates the structure at higher impact velocities is not known. In this analysis, it was assumed that at these higher velocities, the penetration of a multiwall structure depends on the kinetic energy of the projectile. Therefore, it was assumed that the curve defining the minimum mass which penetrates a multiwall structure at these higher velocities can best be approximated by a curve of constant kinetic energy drawn through the highest velocity data point available for the structure. The selection of this penetration criterion was based on laboratory data like that presented in figure 5. The slope of the minimum-mass data curve in figure 5 increases with increased impact velocity. The equation of the line drawn between the two highest velocity data points is of the form $m = k_1 V^{-1.5}$. This double-wall structure was not penetrated when it was struck by a projectile with a mass of $1.9 \times 10^{-2}$ gram at a velocity of 6.8 km/s as indicated by

the arrow in figure 5. This result indicates that the slope of the data curve between 5 and 6.8 km/s would not greatly exceed the slope of the constant-kinetic-energy curve $m = k_2 V^{-2}$ that is drawn through the highest velocity data point. A laboratory data point for the minimum mass which penetrates the thermal barrier and photo-subsystem container at a velocity of 7 km/s was obtained in a hypervelocity impact range at the NASA Manned Spacecraft Center. (See fig. 6.) A separation distance of 0.2 meter was used. In two tests conducted with glass projectiles having a mass of $6.5 \times 10^{-4}$ gram, the thermal barrier and 0.4-mm aluminum sheet used to simulate the photo-subsystem container were completely penetrated. In two tests conducted with glass projectiles having a mass of $8.1 \times 10^{-5}$ gram, one of the projectiles completely penetrated the configuration whereas the other projectile did not penetrate the 0.4-mm aluminum sheet. The conclusion was made from these data that the minimum mass which penetrates the thermal barrier and photo-subsystem container is approximately $8.1 \times 10^{-5}$ gram when the impact velocity is 7 km/s. It was, therefore, assumed in this analysis that all meteoroids with a kinetic energy in excess of 2 joules which strike the Lunar Orbiter spacecraft would penetrate the thermal barrier and photo-subsystem container.

The meteoroid environment which the Lunar Orbiter spacecraft encountered near the moon was assumed to be identical to the near-earth meteoroid environment and was described by the two distributions presented in figure 7. The distribution of meteoroid masses is described by the cumulative mass-flux curve in figure 7(a). This curve is the fit II near-earth meteoroid flux reported in reference 1 and is based primarily on satellite penetration experiments. The distribution of meteoroid velocities is described by the velocity distribution in figure 7(b). This histogram is the corrected meteor velocity distribution of McCrosky and Posen presented in reference 2 and is based on observations of the luminous trails produced by meteoroids in the earth's atmosphere.

The penetration flux calculated for the configuration of the thermal barrier and photo-subsystem container by using the numerical method outlined in figure 3 is $4.2 \times 10^{-9}$ penetration/$m^2$-s. The numerical calculation of the penetration flux is presented in table I.

## FLIGHT DATA FROM THE LUNAR ORBITER SPACECRAFT

### Penetration Flux for the Lunar Orbiter Multiwall Structure

The inner wall of the multiwall structure on the Lunar Orbiter spacecraft is the pressurized photo-subsystem container. Therefore, the monitoring of the internal pressure in the photo subsystem provided data on the penetration flux for the multiwall structure. A meteoroid penetration would cause a loss of pressure. The internal pressure of the photo subsystem was checked many times a day during the photographic missions of

all five Lunar Orbiter spacecraft (that is, the first 30 days of the total mission) and less frequently, typically several days apart, for the extended missions.

In four of the five Lunar Orbiter spacecraft, internal pressure was maintained through the entire mission. Only Lunar Orbiter II experienced a loss of pressure in the photo subsystem. The dates of the major events during the five Lunar Orbiter missions are given in table II. The information was obtained from references 3 to 7. It was estimated in reference 4, from the rate at which the photo subsystem lost pressure, that the area of the leak developed in Lunar Orbiter II was between 0.05 $mm^2$ and 0.3 $mm^2$. A meteoroid penetration could have been responsible for the loss in pressure. Or thermal cycling of the photo subsystem could have caused a crack to develop in a weld seam or could have caused a patch, used to seal a leak discovered at the NASA Kennedy Space Center, to be dislodged. The thermal cycling experienced by Lunar Orbiter II was caused by a malfunction which left the thermal door fully open for the 100 days preceding the sudden loss of pressure in the photo subsystem. Therefore, whether a meteoroid penetration occurred is not clear.

Although an accurate measurement of the penetration flux for the configuration of the thermal barrier and photo-subsystem container was not obtained, some limits can be placed on the penetration flux that would produce either zero or one penetration. If the assumption is made that the distribution of the time intervals between meteoroid penetrations is a Poisson distribution, which appears to be a good approximation from the data presented in reference 8, then the upper and lower limits of the mean penetration flux can be calculated by using the chi-squared distribution in the manner described in reference 8. The expressions for the upper limit $\psi_U$ and the lower limit $\psi_L$ of the 95-percent confidence interval are

$$\psi_L = \frac{\chi^2_{0.025}(2K)}{2A\tau} \tag{4}$$

$$\psi_U = \frac{\chi^2_{0.975}(2K + 2)}{2A\tau} \tag{5}$$

where $K$ is the number of penetrations, $A$ is the area of the structure exposed to the meteoroid environment, and $\tau$ is the exposure time.

The area of the photo-sybsystem container was 1.4 $meters^2$, but shielding of the container by other massive components reduced the effective area exposed to the meteoroid environment to about 0.69 $meter^2$. The total duration of the five Lunar Orbiter missions was $7.5 \times 10^7$ seconds. (See table II.) Thus the exposure $A\tau$ to the meteoroid environment was $5.2 \times 10^7$ $m^2$-s.

If the assumption is made that no meteoroid penetrations occurred through the photo-subsystem container, the upper limit of the penetration flux is

$7.1 \times 10^{-8}$ penetration/$m^2$-s and the lower limit is zero. If the assumption is made that one meteoroid penetration occurred, then the upper limit is $1.1 \times 10^{-7}$ penetration/$m^2$-s and the lower limit is $4.9 \times 10^{-10}$ penetration/$m^2$-s. The statistically small number of penetrations, zero or one, has resulted in a great uncertainty in the value of the mean penetration flux. The calculated penetration flux of $4.2 \times 10^{-9}$ penetration/$m^2$-s is in agreement with the flight results, within the accuracy of the flight data, whether zero or one meteoroid penetration is assumed.

### Penetration Flux for the Lunar Orbiter Single-Wall Meteoroid Detectors

Each of the Lunar Orbiter spacecraft had 20 pressurized cells mounted on the outside of the thermal barrier to measure the penetration flux for single walls in the near-lunar meteoroid environment. The 25-$\mu$m-thick beryllium-copper pressure cells were punctured at a rate equal to one-half the rate observed when the same type detector was flown in the near-earth environment on Explorer XVI. (See refs. 8 and 9.) This result indicates that the near-lunar and near-earth meteoroid environments are not identical and that a correction should be applied to the calculated penetration flux for the thermal barrier and photo-subsystem container because the near-earth meteoroid environment was used in the calculation.

If the difference between the near-lunar and near-earth meteoroid environments is a factor of 2 in the cumulative mass-flux curve, the corrected calculated penetration flux for the thermal barrier and photo-subsystem container is $2.1 \times 10^{-9}$ penetration/$m^2$-s. This corrected calculated penetration flux is in agreement with the flight results, within the accuracy of the data.

## DISCUSSION

### Efficiency Factor for the Lunar Orbiter Multiwall Structure

The reduction in the weight of the meteoroid shielding of a spacecraft which can be obtained by using a multiwall structure can be expressed in terms of the efficiency factor $E$ of the structure. The efficiency factor is defined as

$$E = \frac{t_{eff}}{t_{act}} \tag{6}$$

where $t_{act}$ is the actual total thickness of the various walls, when all walls are constructed of the same material, and $t_{eff}$ is the thickness of a single wall of the given material which has the same penetration flux as the multiwall structure being considered.

For the configuration of the thermal barrier and the photo-subsystem container, the two walls are not the same material. However, the value of $t_{act}$ can be calculated by converting the thermal barrier to an equivalent thickness of aluminum. The equivalent

thickness of aluminum is that thickness which has the same mass per unit area as the thermal barrier. As shown in reference 10, the effectiveness of a meteoroid bumper depends on the mass per unit area and is independent of the bumper material. The value of $t_{act}$ for the Lunar Orbiter multiwall structure is therefore 0.45 mm.

To calculate the value of $t_{eff}$, the penetration flux through single aluminum sheets as a function of the sheet thickness must be known. This relationship, given in reference 11 for the near-earth meteoroid environment, is

$$\log_{10} \psi = -5.966 + 1.364 \log_{10} \frac{t}{2} - 0.683 \log_{10}{}^2 \frac{t}{2} \tag{7}$$

where $\psi$ is the penetration flux in penetrations per meter$^2$-second and $t$ is the aluminum thickness in micrometers. Thus, the penetration flux near the moon is given by

$$\log_{10} 2\psi = -5.966 + 1.364 \log_{10} \frac{t}{2} - 0.683 \log_{10}{}^2 \frac{t}{2} \tag{8}$$

where the factor of 2 for the difference between the penetration fluxes of the near-lunar and near-earth meteoroid environments observed in the Lunar Orbiter and Explorer XVI single-wall penetration experiments has been taken into account. The value of $t_{eff}$ is equal to the value of $t$ obtained by substituting the penetration flux of the thermal barrier and photo-subsystem container into equation (8).

When the limits for the mean penetration flux $\psi_L$ and $\psi_U$ that were derived from the Lunar Orbiter flight data are substituted into equation (8) and when the resultant values of $t_{eff}$ and the value of 0.45 mm for $t_{act}$ are substituted into equation (6), the efficiency factor is found to be greater than 1.4 if no meteoroid penetrations are assumed to have occurred and between 1.1 and 9.4 if one meteoroid penetration is assumed to have occurred. The calculated efficiency factor; that is, the efficiency factor corresponding to the corrected calculated penetration flux of $2.1 \times 10^{-9}$ penetration/m$^2$-s, is 5.9.

Thus, the flight data from the Lunar Orbiter missions indicate that the multiwall structure consisting of the thermal barrier and photo-subsystem container is a more efficient structure in resisting meteoroid penetration than a single aluminum wall of the same mass per unit area. However, it is not possible to estimate from the Lunar Orbiter data how much more efficient the multiwall structure is.

### Other Methods of Calculating Penetration Flux for Multiwall Structures

The method used to calculate the penetration flux of the thermal barrier and photo subsystem provided only a first approximation because the assumption was made that the meteoroid mass and velocity are the only meteoroid parameters which have a first-order effect on the penetration of a multiwall structure. There is reason to believe that the

minimum mass that penetrates a multiwall structure also depends on the density of the meteoroid and the impact angle. A calculation of the penetration flux which includes these meteoroid parameters is indicated by

$$\psi_c = \int_{\theta=0}^{\pi/2} d\theta \int_{\rho=0}^{\infty} d\rho \int_{V=0}^{\infty} dV \int_{m=f(\theta,\rho,V)}^{\infty} \frac{\partial \phi}{\partial m} g(V)h(\rho)i(\theta)\, dm \qquad (9)$$

where $m = f(\theta,\rho,V)$ is the penetration criterion for the structure, $h(\rho)$ is the meteoroid density probability density function, and $i(\theta)$ is the meteoroid impact-angle probability density function. The penetration criterion and the distributions of meteoroid densities and impact angles required to perform the calculation indicated by equation (9) have not been established. Even more complete methods of calculating the meteoroid penetration flux might include the shape and material properties of the meteoroids. Multiwall penetration-flux data obtained in space are needed to determine the complexity required in the method of calculating penetration flux in order to obtain the desired accuracy.

## Experimental Requirements to Demonstrate Accuracy of a Method of Calculating Penetration Flux

It is desirable to have a method of predicting meteoroid penetration flux for a multiwall spacecraft structure with an accuracy appropriate to the spacecraft mission. To demonstrate that a method has the desired accuracy, flight experiments must be conducted in which several penetrations of a multiwall structure are obtained.

The multiwall penetration-flux data obtained from the Lunar Orbiter missions were not adequate to provide a check for the method of calculating the penetration flux because the number of meteoroid penetrations that occurred was too small. If the loss of pressure on Lunar Orbiter II is assumed to have been caused by a meteoroid penetration, the upper and lower limits of the 95-percent confidence interval for the penetration flux differ by a factor of 220. Therefore, it is impossible to demonstrate with these data that the calculated penetration flux is accurate to more than a factor of 14.8 $\left(\text{that is, } \sqrt{220}\right)$. It is, in general, impossible to show that a calculation is accurate to within a factor of $N$ if the uncertainty in the flight data exceeds a factor of $N^2$. A calculated penetration flux is said to be accurate to within a factor of $N$ if $\frac{\psi_c}{N} \leqq \psi \leqq N\psi_c$, where $\psi_c$ is the calculated penetration flux and $\psi$ is the actual mean penetration flux.

The great uncertainty in the mean penetration flux for the configuration of the thermal barrier and photo-subsystem container as determined from the flight data of the Lunar Orbiter missions is a consequence of having obtained zero or only one penetration. If, for instance, the missions of all five Lunar Orbiters could have been extended until a meteoroid penetration of the thermal barrier and photo-subsystem container was detected

for each spacecraft, the penetration flux of the configuration would have been measured with 95-percent confidence to within a factor of 7.2. It might then have been possible to demonstrate that the method of calculating penetration flux was accurate to within a factor of 2.7 $\left(\text{that is, } \sqrt{7.2}\right)$.

The designer of a spacecraft must determine the accuracy that is required in the calculation of the penetration flux for the spacecraft. The designer is usually interested in the reliability of the spacecraft, which in the case of meteoroids might be the probability that the spacecraft will not be penetrated by a meteoroid. The probability of no penetrations $P_0$ is

$$P_0 = e^{-\psi A \tau} \tag{10}$$

where $A$ is the area of the spacecraft structure exposed to the meteoroid environment, $\tau$ is the time of exposure to the environment, and $\psi$ is the mean penetration flux. The first three columns of table III show the uncertainty in $P_0$ which results from an uncertainty in the calculated penetration flux. In column ① are listed the accuracy factors for the calculated penetration flux. Column ② shows the limits of uncertainty in $P_0$ if the calculated penetration flux gives $P_0 = 0.90$, and column ③ shows the limits of uncertainty in $P_0$ if calculated penetration flux gives $P_0 = 0.99$.

The uncertainty factor in the measurement of the penetration flux $\psi_U/\psi_L$ which can be tolerated in a flight experiment conducted to demonstrate that a method of calculating penetration flux is accurate to within a factor of $N$ is in the interval

$$\frac{N}{Z} \leqq \frac{\psi_U}{\psi_L} \leqq N^2 \qquad (Z \leqq N) \tag{11}$$

where $Z$, the error factor in the method of calculating the penetration flux, is defined as $Z = \frac{\psi}{\psi_c}$ when $\psi > \psi_c$ and $Z = \frac{\psi_c}{\psi}$ when $\psi_c > \psi$. The actual mean penetration flux is assumed to be between $\psi_U$ and $\psi_L$, which it should be for 95 percent of the experiments.

If the method of calculating the penetration flux is exactly correct ($Z = 1$), then the value of $\psi_U/\psi_L$ required to demonstrate that the method of calculating penetration flux is accurate to within a factor of $N$ is somewhere in the range $N \leqq \frac{\psi_U}{\psi_L} \leqq N^2$, depending on the results of the particular flight experiment. If the method of calculating the penetration flux is not exactly correct ($Z \neq 1$), greater demands are placed on the accuracy that is required in a flight experiment. If $Z > N$, it is, of course, impossible to show that $Z \leqq N$, except perhaps in those 5 percent of the experiments in which the actual mean penetration flux does not fall in the 95-percent confidence interval.

The limits of $\psi_U/\psi_L$ required in a flight experiment to demonstrate that $Z \leqq N$ are shown in columns 4 and 5 in table III for $Z = 1$. The corresponding number of penetrations needed in an experiment to obtain the desired experimental accuracy is also shown in columns 6 and 7 in table III.

To illustrate the use of table III, take as an example the sixth row of numbers. Suppose that an accuracy factor of 2 in the penetration flux for a given structure is acceptable (column ①). The uncertainty in the probability of no penetrations for the structure would be 0.82 to 0.95 if the calculated penetration flux gives $P_0 = 0.90$ (column ②) and 0.980 to 0.995 if the calculated penetration flux gives $P_0 = 0.990$ (column ③). If it is desired to demonstrate with a flight experiment that the calculated penetration flux is in reality accurate to within a factor of 2 (column ①), a flight experiment must be performed in which the measured penetration flux is accurate to within a factor of 2 (column ④) to 4 (column ⑤). To obtain these accuracies in a flight experiment requires that a minimum of 10 (column ⑥) to 35 (column ⑦) penetrations be obtained.

## CONCLUDING REMARKS

The method used to calculate the penetration flux for the multiwall structure consisting of the thermal barrier and the photo-subsystem container on the Lunar Orbiter spacecraft has been presented.

The calculation of the efficiency factor showed that the multiwall structure provided better protection against meteoroids than a single aluminum wall with the same mass per unit area. The calculated efficiency factor was 5.9. The flight data from the five Lunar Orbiter missions verified that the multiwall structure was more effective than a single aluminum wall of the same mass per unit area, but the data were not adequate to determine the value of the multiwall efficiency factor.

Methods of calculating the penetration flux in multiwall structures must be checked by flight experiments in which several penetrations of a multiwall structure are obtained. For instance, if it is desired to demonstrate with a flight experiment that a method of calculating the penetration flux is accurate to within a factor of 2, an experiment must be conducted in which a minimum of 10 to 35 penetrations are obtained.

Langley Research Center,
National Aeronautics and Space Administration,
Langley Station, Hampton, Va., July 7, 1969.

## REFERENCES


1. Naumann, Robert J.: The Near-Earth Meteoroid Environment. NASA TN D-3717, 1966.

2. Clough, Nestor; and Lieblein, Seymour: Significance of Photographic Meteor Data in the Design of Meteoroid Protection for Large Space Vehicles. NASA TN D-2958, 1965.

3. Boeing Co.: Lunar Orbiter I – Extended-Mission Spacecraft Subsystem Performance. NASA CR-870, 1967.

4. Boeing Co.: Lunar Orbiter II – Extended-Mission Spacecraft Operations and Subsystem Performance. NASA CR-1141, 1968.

5. Boeing Co.: Lunar Orbiter III – Extended-Mission Spacecraft Operations and Subsystem Performance. NASA CR-1109, 1968.

6. Boeing Co.: Lunar Orbiter IV – Extended-Mission Spacecraft Operations and Subsystem Performance. NASA CR-1092, 1968.

7. Boeing Co.: Lunar Orbiter V – Extended-Mission Spacecraft Operations and Subsystem Performance. NASA CR-1142, 1968.

8. Hastings, Earl C., Jr., compiler: The Explorer XVI Micrometeoroid Satellite – Supplement III, Preliminary Results for the Period May 27, 1963, Through July 22, 1963. NASA TM X-949, 1964.

9. Gurtler, C. A.; and Grew, Gary W.: Meteoroid Hazard Near Moon. Science, vol. 161, no. 3840, Aug. 2, 1968, pp. 462-464.

10. Humes, Donald H.: Influence of the Bumper and Main Wall Material on the Effectiveness of Single Meteoroid Bumpers. NASA TN D-3104, 1965.

11. O'Neal, Robert L., compiler: The Explorer XXIII Micrometeoroid Satellite – Description and Results for the Period November 6, 1964, Through November 5, 1965. NASA TN D-4284, 1968.

TABLE I.- CALCULATION OF PENETRATION FLUX FOR CONFIGURATION OF THERMAL BARRIER AND PHOTO-SUBSYSTEM CONTAINER

| Velocity interval, km/s | Minimum mass that penetrates structure, g | Cumulative flux for minimum mass, no./$m^2$-s | Fraction of meteoroids in velocity interval | Calculated penetration flux, penetrations/$m^2$-s |
|---|---|---|---|---|
| 10 to 15 | $25 \times 10^{-6}$ | $1.4 \times 10^{-9}$ | 0.333 | $4.66 \times 10^{-10}$ |
| 15 to 20 | 13 | 2.6 | .317 | 8.24 |
| 20 to 25 | 7.7 | 4.4 | .161 | 7.08 |
| 25 to 30 | 5.2 | 6.4 | .077 | 4.93 |
| 30 to 35 | 3.7 | 9.0 | .041 | 3.69 |
| 35 to 40 | 2.8 | 11 | .025 | 2.75 |
| 40 to 45 | 2.2 | 15 | .015 | 2.25 |
| 45 to 50 | 1.7 | 19 | .006 | 1.14 |
| 50 to 55 | 1.4 | 22 | .004 | .88 |
| 55 to 60 | 1.2 | 26 | .006 | 1.56 |
| 60 to 65 | 1.0 | 30 | .006 | 1.80 |
| 65 to 70 | .86 | 34 | .006 | 2.04 |
| 70 to 75 | .75 | 38 | .003 | 1.14 |
| Total . . . . . | | | | $42 \times 10^{-10}$ |

TABLE II.- DATES OF MAJOR EVENTS DURING LUNAR ORBITER MISSIONS

| Lunar Orbiter spacecraft | Date of – | | | | Experiment duration, days (a) |
|---|---|---|---|---|---|
| | Launch | Injection into lunar orbit | Loss of pressure | Last communication | |
| I | Aug. 10, 1966 | Aug. 14, 1966 | ---------- | Oct. 29, 1966 | 76 |
| [b]II | Nov. 6, 1966 | Nov. 10, 1966 | Sept. 1, 1967 | Oct. 11, 1967 | [c]295 |
| III | Feb. 5, 1967 | Feb. 8, 1967 | ---------- | Oct. 9, 1967 | 243 |
| IV | May 4, 1967 | May 8, 1967 | ---------- | July 17, 1967 | 70 |
| V | Aug. 1, 1967 | Aug. 5, 1967 | ---------- | Jan. 31, 1968 | 179 |

[a]Time from injection into lunar orbit to time when communication was discontinued unless otherwise noted.

[b]Thermal door was opened between Feb. 17, 1967, and Feb. 19, 1967, and remained open for duration of mission.

[c]Time from injection into lunar orbit to time when photo subsystem began to lose pressure.

TABLE III.- EXPERIMENTAL REQUIREMENTS TO DEMONSTRATE ACCURACY OF METHOD OF CALCULATING PENETRATION FLUX (Z = 1)

| ① | ② | ③ | ④ | ⑤ | ⑥ | ⑦ |
|---|---|---|---|---|---|---|
| Accuracy factor N of calculated penetration flux $\left(\frac{\psi_c}{N} \leq \psi \leq N\psi_c\right)$ | Uncertainty in probability of no penetrations for – | | Uncertainty factor of measured penetration flux | | Number of penetrations required in experiment for – | |
| | $\psi_c \rightarrow P_o = 0.90$ | $\psi_c \rightarrow P_o = 0.990$ | $(\psi_U/\psi_L)_{min}$ | $(\psi_U/\psi_L)_{max}$ | $(\psi_U/\psi_L)_{max}$ | $(\psi_U/\psi_L)_{min}$ |
| 1.0 | 0.90 to 0.90 | 0.990 to 0.990 | 1.0 | 1.00 | ∞ | ∞ |
| 1.2 | .89 to .92 | .988 to .992 | 1.2 | 1.44 | 116 | 460 |
| 1.4 | .87 to .93 | .986 to .993 | 1.4 | 1.96 | 37 | 137 |
| 1.6 | .85 to .94 | .984 to .994 | 1.6 | 2.56 | 20 | 71 |
| 1.8 | .84 to .95 | .982 to .994 | 1.8 | 3.24 | 13 | 48 |
| 2 | .82 to .95 | .980 to .995 | 2 | 4 | 10 | 35 |
| 3 | .74 to .97 | .970 to .997 | 3 | 9 | 5 | 15 |
| 4 | .67 to .98 | .961 to .998 | 4 | 16 | 3 | 10 |
| 5 | .61 to .98 | .951 to .998 | 5 | 25 | 3 | 8 |
| 10 | .37 to .99 | .904 to .999 | 10 | 100 | 2 | 4 |
| 15 | .22 to .99 | .861 to .999 | 15 | 225 | 1 | 3 |

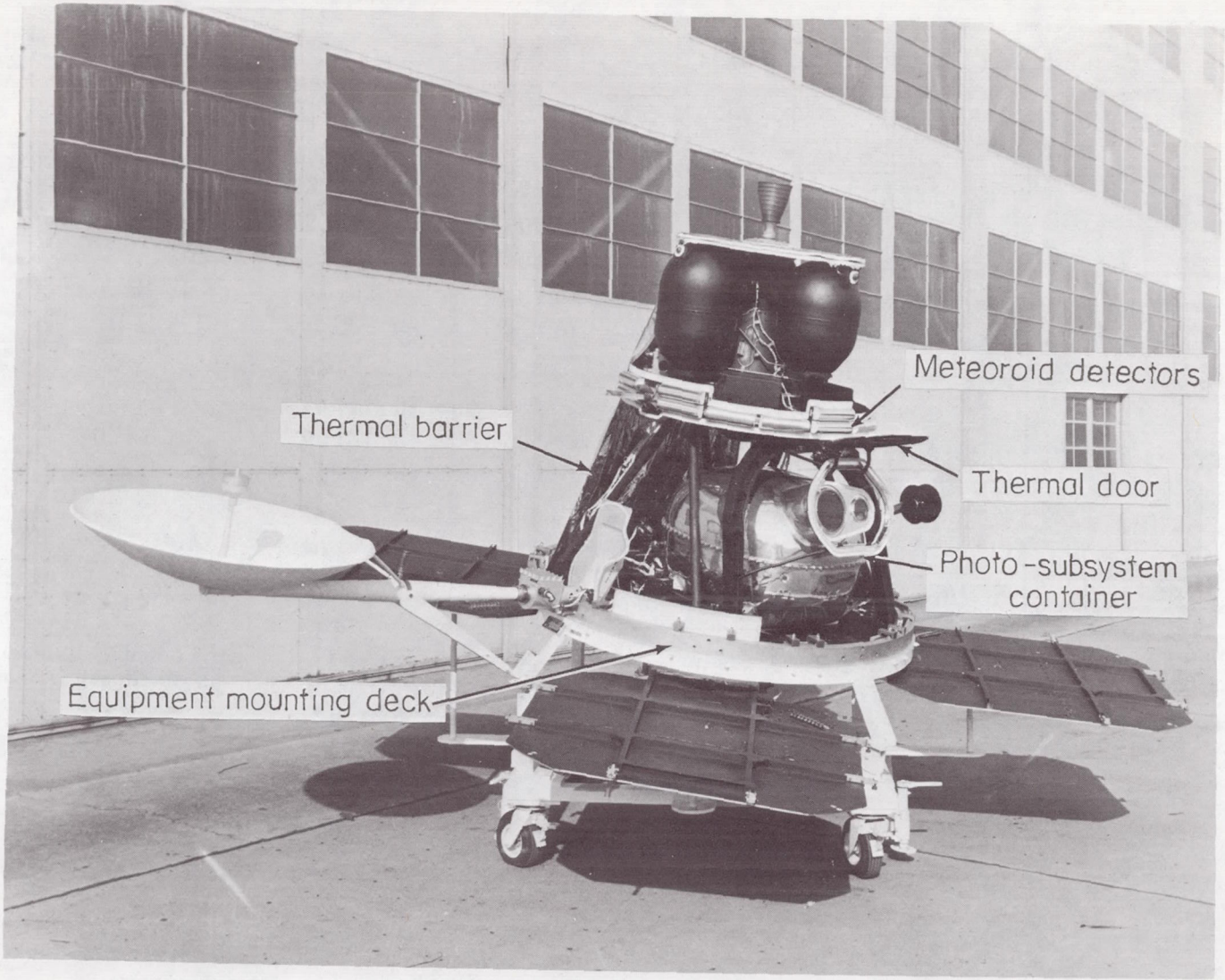


Figure 1.- Lunar Orbiter spacecraft.

L-67-9153

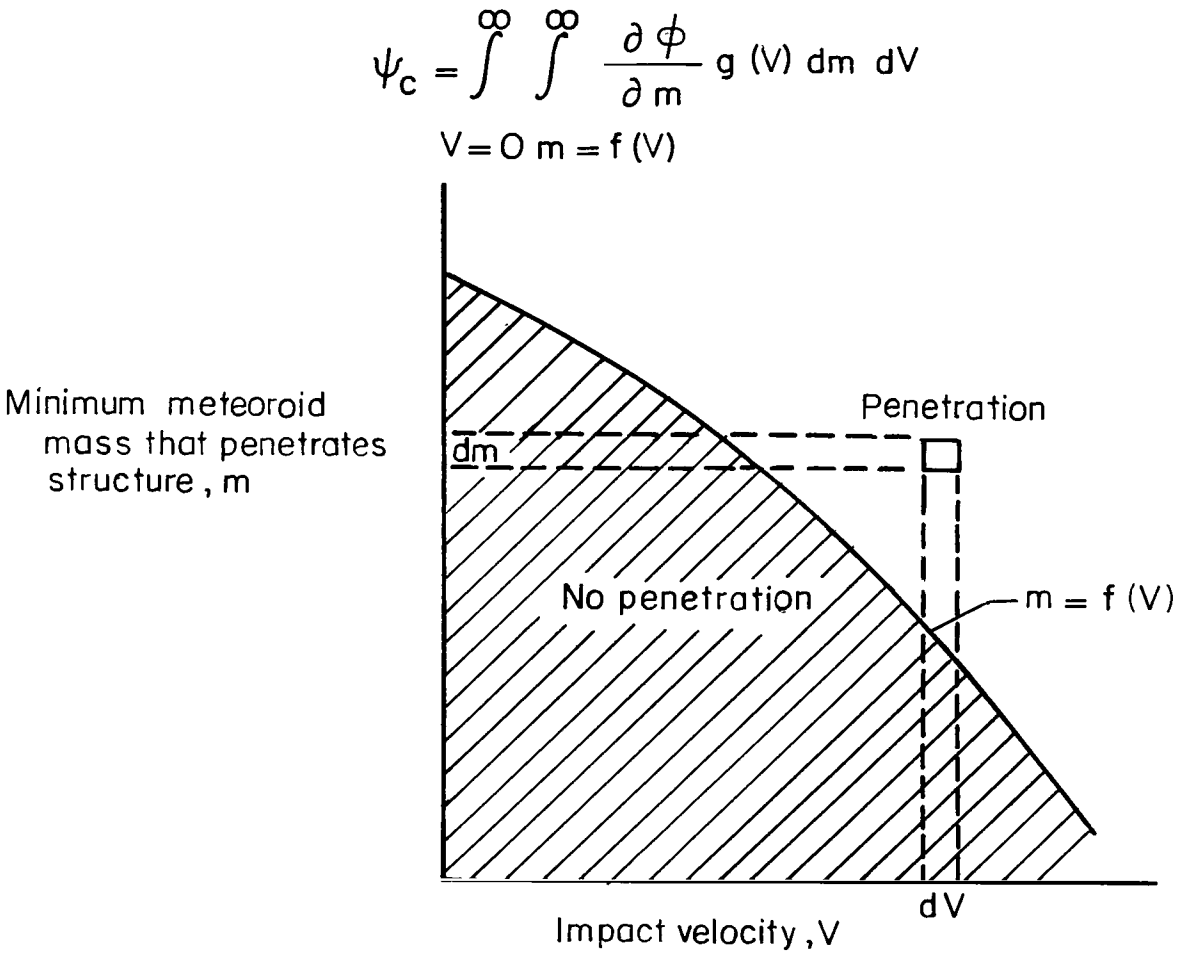


Figure 2.- Method of calculating penetration flux for a multiwall structure.

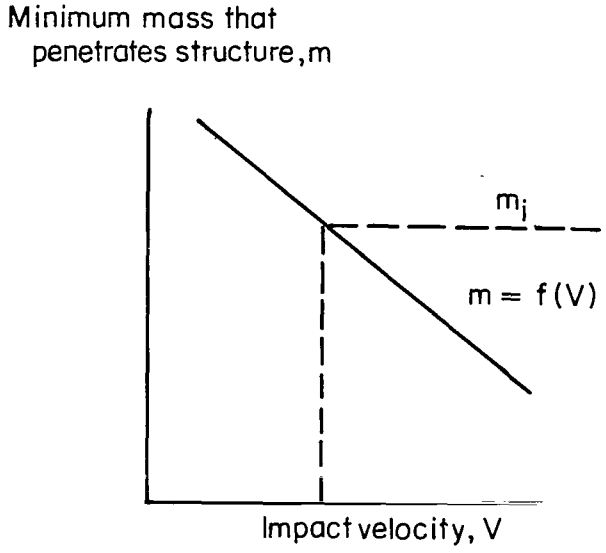


(a) Penetration criterion for structure.

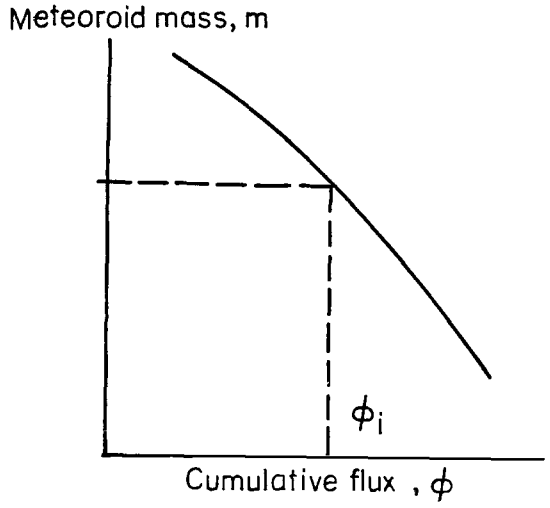


(b) Cumulative mass-flux curve.

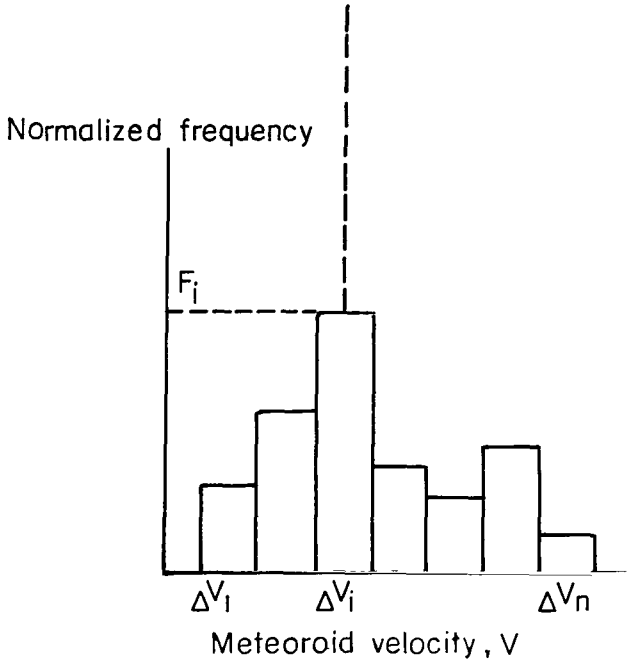


$$\psi_i = F_i \phi_i$$

$$\psi_c = \sum_{i=1}^{n} F_i \phi_i$$

(c) Velocity distribution.

Figure 3.- Numerical method of calculating penetration flux for a multiwall structure.

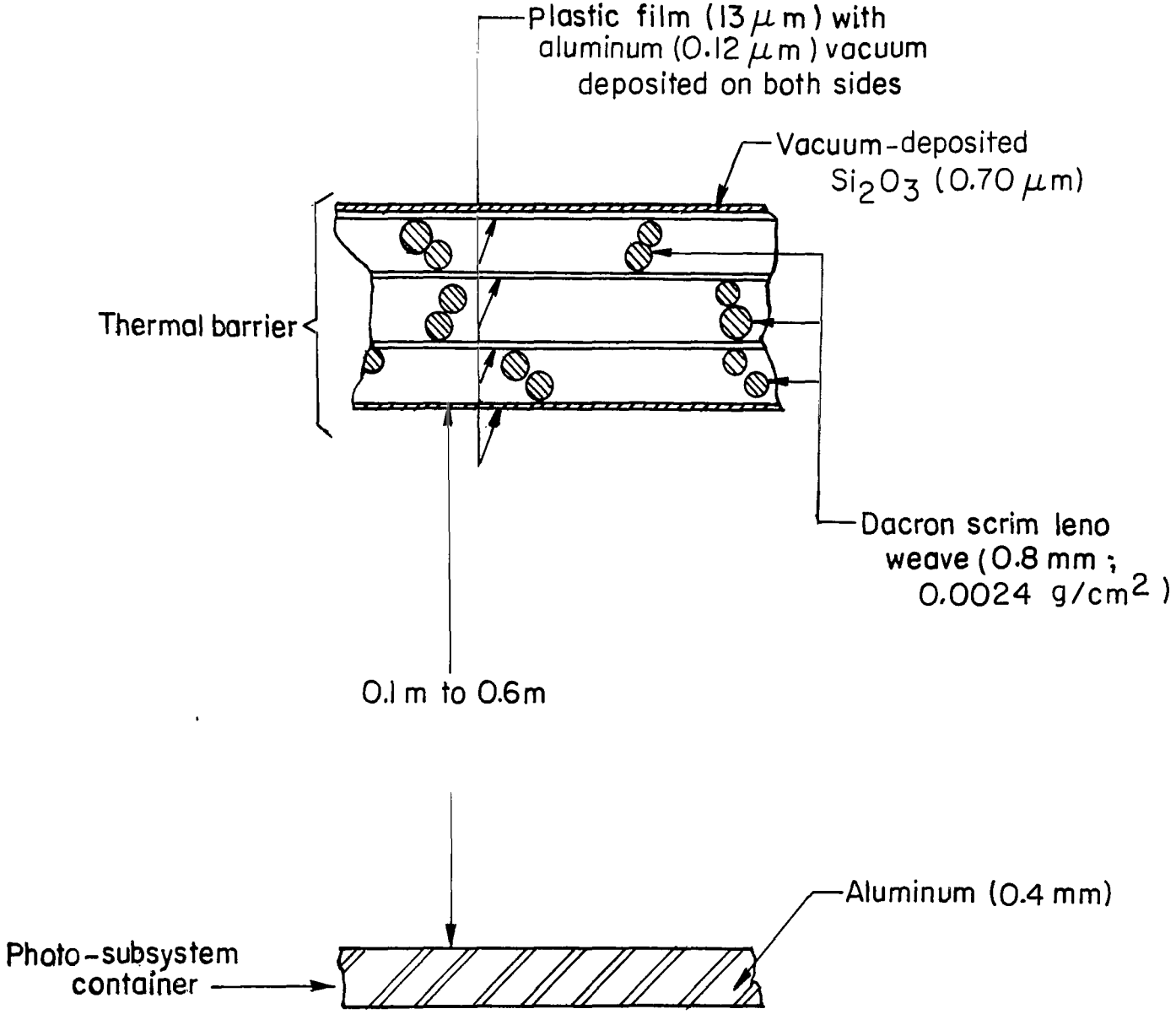


Figure 4.- Sketch of thermal-barrier material and photo-subsystem-container material.

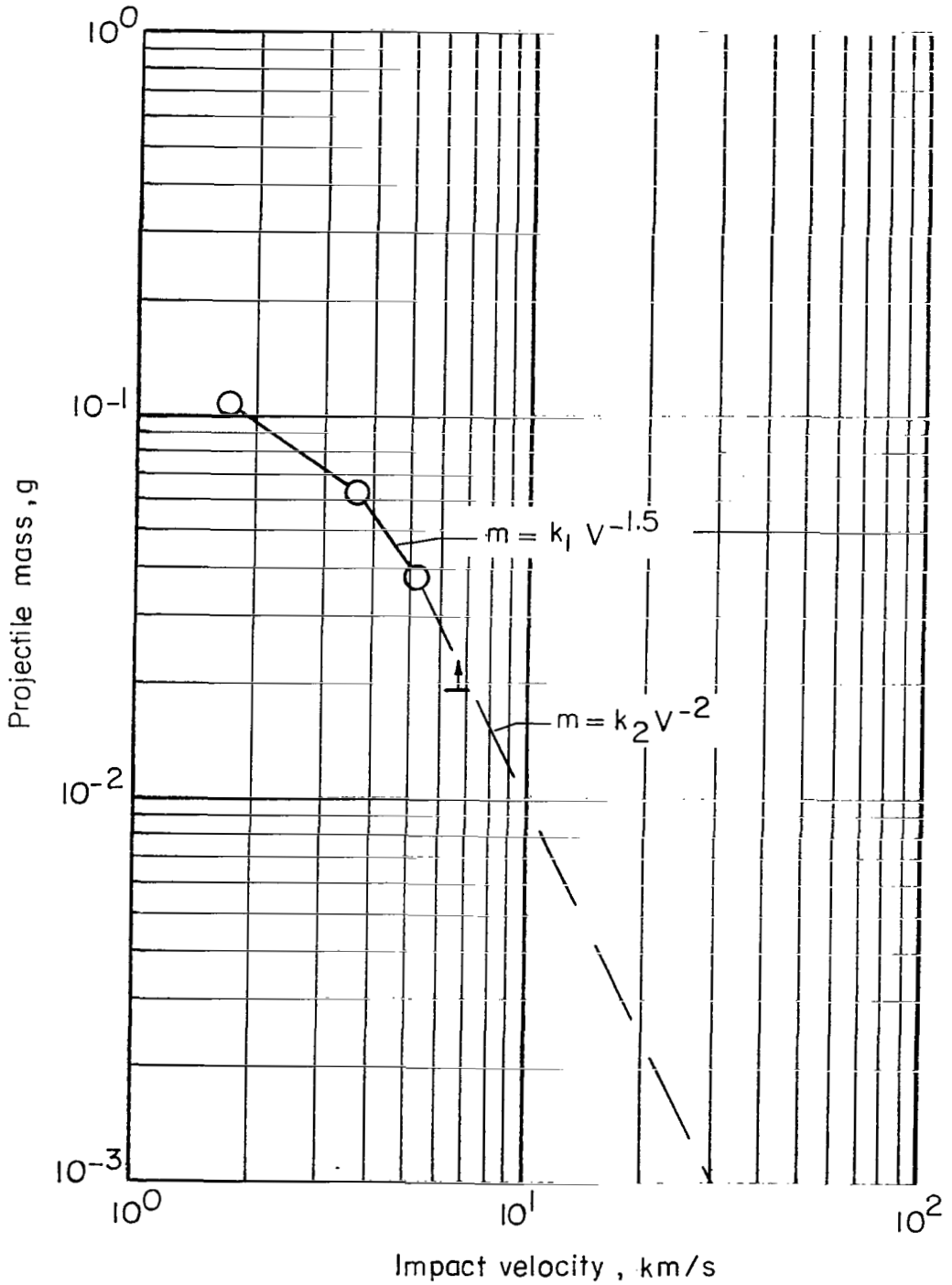


Figure 5.- Minimum-penetrating-mass curve for double-wall aluminum structure. Aluminum sheet (0.81 mm) as meteoroid bumper; aluminum sheet (1.60 mm) as main wall; 25-mm spacing; nylon-sphere projectiles. Arrow indicates no penetration for projectile of $1.9 \times 10^{-2}$ gram with impact velocity of 6.8 km/s.

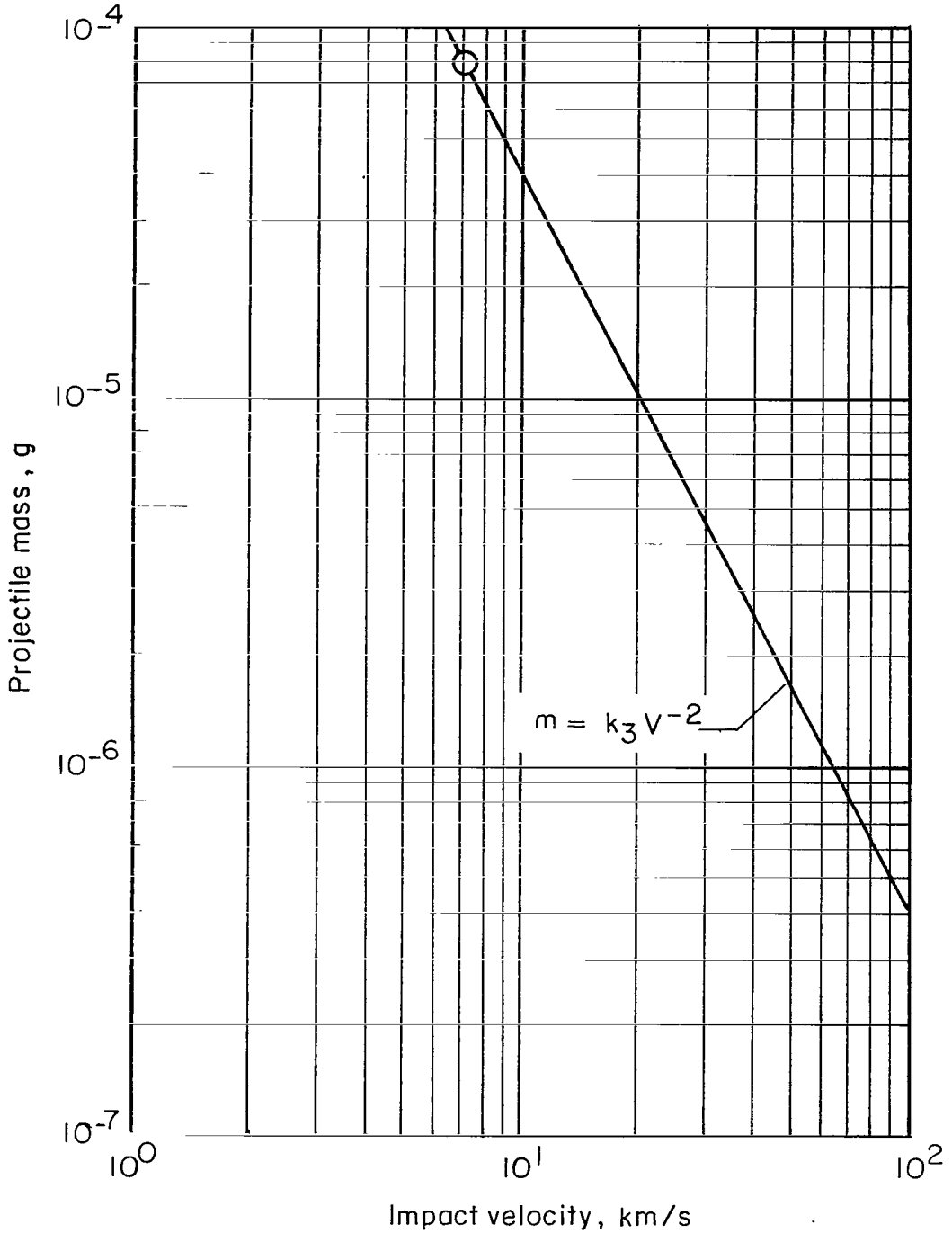


Figure 6.- Penetration criterion for configuration of thermal barrier and photo-subsystem container. Thermal barrier as meteoroid bumper; photo-subsystem container as main wall; 0.2-meter spacing; glass-sphere projectiles. Data point obtained in hypervelocity impact range at NASA Manned Spacecraft Center.

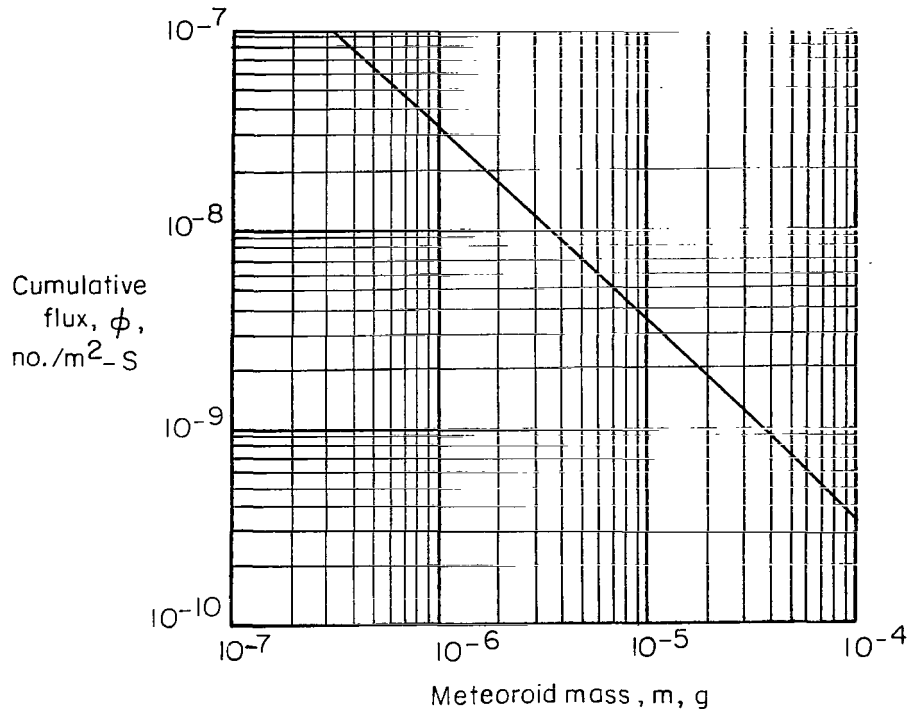


(a) Cumulative mass-flux curve for meteoroids. Fit II flux from reference 1.

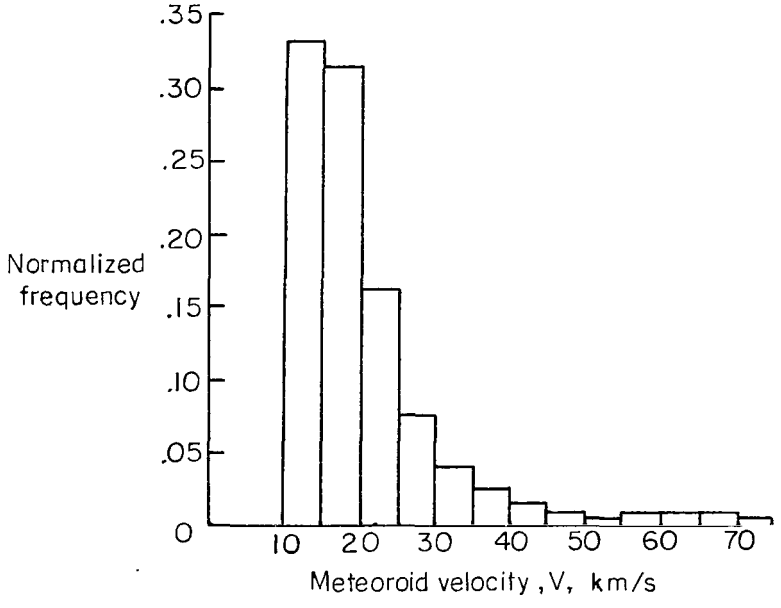


(b) Velocity distribution of meteoroids. Meteor data from reference 2.

Figure 7.- Model of near-earth meteoroid environment.



NASA-Langley, 1969 —— 32 L-6609

NATIONAL AERONAUTICS AND SPACE ADMINISTRATION
WASHINGTON, D. C. 20546

OFFICIAL BUSINESS

FIRST CLASS MAIL

POSTAGE AND FEES PAID
NATIONAL AERONAUTICS AND
SPACE ADMINISTRATION



*"The aeronautical and space activities of the United States shall be conducted so as to contribute . . . to the expansion of human knowledge of phenomena in the atmosphere and space. The Administration shall provide for the widest practicable and appropriate dissemination of information concerning its activities and the results thereof."*

—NATIONAL AERONAUTICS AND SPACE ACT OF 1958

# NASA SCIENTIFIC AND TECHNICAL PUBLICATIONS

TECHNICAL REPORTS: Scientific and technical information considered important, complete, and a lasting contribution to existing knowledge.

TECHNICAL NOTES: Information less broad in scope but nevertheless of importance as a contribution to existing knowledge.

TECHNICAL MEMORANDUMS: Information receiving limited distribution because of preliminary data, security classification, or other reasons.

CONTRACTOR REPORTS: Scientific and technical information generated under a NASA contract or grant and considered an important contribution to existing knowledge.

TECHNICAL TRANSLATIONS: Information published in a foreign language considered to merit NASA distribution in English.

SPECIAL PUBLICATIONS: Information derived from or of value to NASA activities. Publications include conference proceedings, monographs, data compilations, handbooks, sourcebooks, and special bibliographies.

TECHNOLOGY UTILIZATION PUBLICATIONS: Information on technology used by NASA that may be of particular interest in commercial and other non-aerospace applications. Publications include Tech Briefs, Technology Utilization Reports and Notes, and Technology Surveys.

*Details on the availability of these publications may be obtained from:*

SCIENTIFIC AND TECHNICAL INFORMATION DIVISION

NATIONAL AERONAUTICS AND SPACE ADMINISTRATION

**Washington, D.C. 20546**